Radiation Characteristics of a Microstrip Patch Over an Electromagnetic Bandgap Surface

Jing Liang, *Student Member, IEEE*, and Hung-Yu David Yang, *Fellow, IEEE*

***Abstract*—Radiation characteristics of a microstrip patch over an electromagnetic bandgap (EBG) substrate are investigated in this paper. This paper focuses on a mushroom-type EBG structure, although the design is applicable to various EBG profiles. The patch antenna is modeled as a half-wavelength resonator of an EBG-loaded microstrip transmission line. Through a full-wave eigenmode analysis of a microstrip line on an EBG structure, it is found that the resonant patch will not see a high-impedance surface (HIS), but rather it is coupled to the EBG structure as an open cavity resonator. Due to strong near-field coupling, the propagation characteristics including the bandgap zones are very different with or without the patch cover. The use of an EBG structure as a bulk material for antennas is seen inappropriate. The EBG surface is found to have the effect of reducing the patch resonant length and bandwidth. A prototype of a microstrip line proximity fed to a patch antenna is fabricated and tested to verify the analysis.**

***Index Terms*—Electromagnetic bandgap (EBG), high-impedance surface (HIS), microstrip patch antenna, periodic microstrip line.**

I. Introduction

With the rapid growth of wireless markets [mobile communication, wireless local area network (WLAN) networking, global positioning system (GPS) services, and radio-frequency identification (RFID) applications], radio-frequency (RF) engineers are facing continuing challenges of small-volume, wide-bandwidth, power efficient, and low-cost system designs. A low-profile, small-size antenna integrated into RF front ends with sufficient bandwidth is essential in wireless systems. Several techniques have been employed to achieve this objective: cutting slots on radiation patch, inserting shorting pins, and meandering electric current paths on the radiation patch [1]. Metamaterials, including electromagnetic bandgap (EBG) structures [2], [3], double negative (DNG) materials [4], [5], and left-handed materials (LHM) [6]–[8], have been well investigated lately. Their novel electromagnetic characteristics have found useful applications in antennas and microwave circuits. EBG printed circuit structures are thin composite dielectric layers with periodic metallic patterns (usually backed by a metal ground plane), and have one or multiple frequency bandgaps in which no substrate mode can exist. This unique property has been applied to design antenna systems with a better gain and efficiency, lower sidelobes and backlobe levels, and better isolations among array elements, by suppressing surface wave mode [9]–[11]. An EBG surface is found equivalent to a perfect magnetic conductor for an incident plane wave in a certain frequency bands in which the phase of the reflection coefficient is close to 0°. This equivalent artificial magnetic conductor (AMC) was discussed extensively in the literatures, for example, in [12]–[14]. The AMC properties with potential applications in low-profile dipole/monopole antenna were discussed [15]–[17].

The EBG substrate has been applied to alleviate some drawbacks of conventional microstrip antennas. Mushroom-like EBG, uniplanar photonic bandgap (PBG), or other metamaterial textures are used to reduce the antenna size [18]–[22]. Microstrip antennas over metamaterial substrates are found to have a larger bandwidth [23], [24].

In this paper, radiation characteristics including return loss, gain, and radiation pattern of a rectangular patch antenna over an EBG substrate are investigated. The aim is to characterize the patch antenna properties in the presence of the EBG surface. Although the simulation of the entire antenna structure is readily available with commercial full-wave solvers, this paper focuses on the design based on the dispersion diagram of a metal-strip transmission line above the EBG surface. An accurate modal analysis of an EBG-loaded microstrip line using the Ansoft high-frequency structure simulator (HFSS, Ansoft, Pittsburgh, PA) is applied to determine the patch resonant length and study the characteristics of the patch radiation mode. The modal analysis can be simplified with a good accuracy to a parallel-plate modal analysis when the patch is sufficiently wide. Subsequently, the resonant frequency of the patch antenna on top of an EBG surface is determined using 3-D full-wave simulations (Zeland IE3D, Zeland Software, Inc., Fremont, CA). This resonant frequency is compared against the frequency from the modal analysis to confirm the validity of both simulations. In particular, mushroom-like EBG textures are investigated. The EBG substrate effects to a patch antenna on top are studied parametrically. The first transmission line bandgap which determines the upper frequency limit of the antenna mode is also characterized. A prototype of a patch antenna on top of an EBG substrate fed by an electromagnetically coupled microstrip line is fabricated and tested. The measured results show good agreement with theoretical prediction.

II. Modal Analysis of an EBG-Loaded Microstrip Line

A rectangular microstrip patch antenna is often treated as a half-wavelength open-circuit resonator. Therefore, a modal analysis of a microstrip line could provide the necessary design information. The example under investigation is the mushroom EBG structure consisting of planar arrays of rectangular patches, each with a shorting pin. Assuming wave propagation along the principal direction, the modal analysis using HFSS (Ansoft finite element solver) is an eigenvalue problem with the

Manuscript received October 31, 2006; revised January 27, 2007.

The authors are with the Department of Electrical and Computer Engineering, University of Illinois at Chicago, Chicago, IL 60607 USA (e-mail: hyang@ece.uic.edu).

Digital Object Identifier 10.1109/TAP.2007.898633

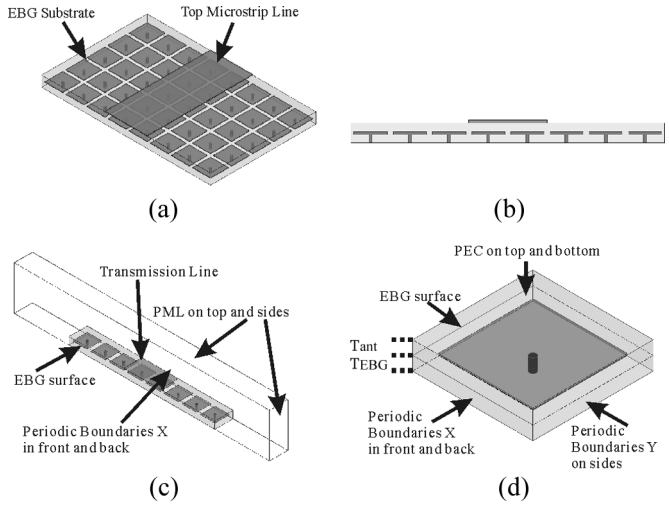

Fig. 1. Microstrip line on an EBG structures: (a) perspective view, (b) cross-section view, (c) FCS-EM model, and (d) UC-EM model.

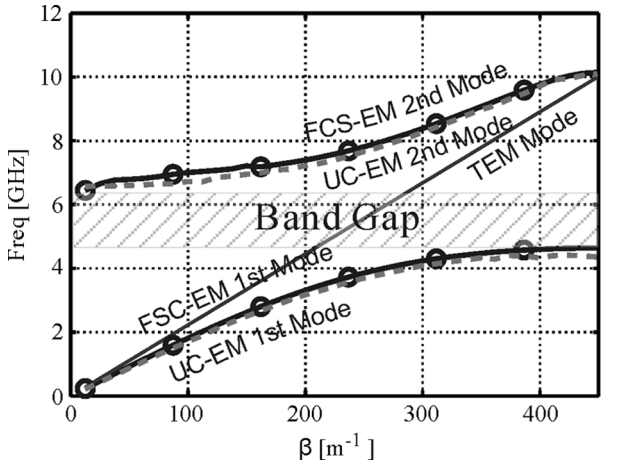

Fig. 2. EBG microstrip-line dispersion diagram and the TEM mode of a parallel plate (removing the mushroom). Circle line is the FCS analysis and dashed line the UC analysis.

geometry of a section of a microstrip line on top of a mushroom EBG structure, as shown in Fig. 1. This modal analysis for the propagation constant and field distributions provides useful physical insights of the patch and EBG coupling and the patch resonant mode.

In HFSS simulation setup, as shown in Fig. 1(c), perfect-matching-layers (PML) boundaries are placed a quarter wavelength away from the substrate sidewalls (in parallel) and also a wavelength above the microstrip line, to mimic the structure of a microstrip on top of an EBG surface. The geometry is periodic in the propagation direction except a phase change and periodic boundaries are placed in the front and back of the simulation box. Assigning a certain phase difference $\Delta\phi$ along the propagation direction, the eigenvalues are the allowable frequencies f. The dispersion diagram can be obtained by varying $\Delta\phi$ from 0° to 180°. $\Delta\phi$ is the phase change along a unit-cell (UC) microstrip length and is equal to the propagation constant β times the UC length. The dispersion diagrams reveal the passbands and the stopbands of the guided waves. Since this approach considers all the EBG substrate microstrip line transverse structure, it is also defined as the full cross-section eigenmode (FCS-EM) modal analysis.

An example of the dispersion diagram of a patch cover EBG structure is shown in Fig. 2. The propagation is along a main axis of the EBG patch. The UC is 7 mm $\times$ 7 mm and the patch is 4.5 mm $\times$ 4.5 mm. The vias at the patch center have a radius of 0.2 mm. The substrate height is 1.5748 mm (62 mil) filled with FR4 material ($\varepsilon_r = 4.6$ and loss tangent 0.01 according to manufacturer data). The EBG patch arrays are in the middle of the cavity. The circle lines in Fig. 2 are the FCS modal analysis of an EBG-loaded microstrip line and the solid line is the TEM mode of parallel plates (removing the mushroom). The transmission line width is 31.6 mm. As a note, when the patch cover is removed, the equivalent AMC spectrum ranges from 12.95 to 16.47 GHz, below which the guided-wave is in the stopband zone (high-pass characteristics). Without a patch cover, the bandgap is due to mode suppression (TM substrate mode). In contrast, the bandgap of the mushroom-like EBG structure with top PEC patch is due to Brag diffraction and the structure has low-pass characteristics. The patch antenna should operate in the slow-wave propagation region below the bandgap (below 4.41 GHz shown in Fig. 2), where it is found that the E field is vertically polarized both above and below the EBG surface similar to a normal microstrip patch mode. Furthermore, at a given resonant frequency, β found from Fig. 2 will determine the patch length (about a half wavelength). It is observed from Fig. 2 that the guided wavelength (about half patch antenna length) could be much reduced in an EBG structure. This observation can be explained though a transmission line theory. The EBG structure enhances the slow-wave factor (larger β) by capacitive loadings from the EBG conductive plate edge and inductive loadings from the shorting vias to the transmission line. Furthermore, the lower and upper bounds of the bandgap frequency are also determined by the equivalent capacitance and inductance per UC introduced by the EBG structure. Another interesting observation from Fig. 2 is that the top metal cover and the EBG structure underneath are coupled together as one guided-wave structure. The equivalent AMC will not be seen by the top metal plate (a patch antenna). Hence, it theoretically explains why the AMC effects cannot be found in the patch antenna design in [25].

A parallel-plate waveguide cavity model is often used in a rectangular microstrip patch antenna design, particularly for a large patch on an electrically thin substrate. Similarly, a cavity model is found useful here in the design of a patch antenna above an EBG surface if the electric fields are mostly in vertical direction confined inside the patch. As a first-order approximation, the antenna structure is treated as a rectangular section (with both planar directions open-circuited) of a parallel-plate structure with embedded EBG structures. Therefore, a modal analysis could be applied to a thin infinitely large parallel-plate waveguide with an EBG UC sandwiched in between. In this modal analysis, a UC is surrounded by four periodic boundaries as shown in Fig. 1(d). Hence it is also defined as unit-cell eigenmode (UC-EM) modal analysis. The results based on a UC-EM analysis are also shown in Fig. 2. It is seen that the agreement between FCS-EM and a UC-EM modal analysis is very good. This observation confirms the cavity nature of the antenna EBG structure.

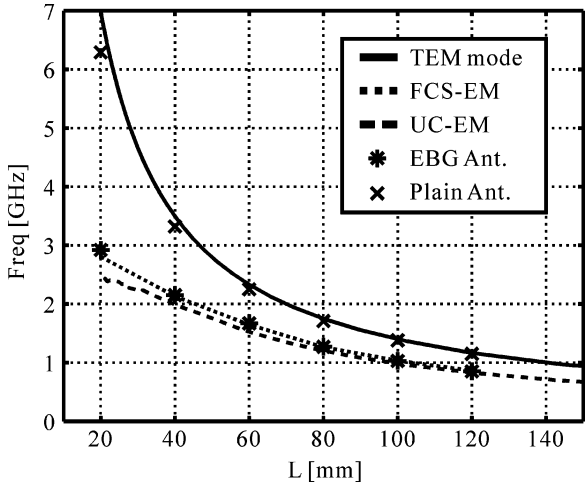

Fig. 3. Resonant length (L) of a square patch antenna. Solid line: no EBG surface. Dashed line: UC modal analysis. Dotted line: FCS modal analysis. Asterisk and cross marks are from IE3D full antenna simulations with and without EBG surface, respectively.

III. Model Validation

The validity of the modal approach for the design of a patch antenna with an EBG surface underneath is further investigated through a full-wave 3-D numerical simulation of an EBG loaded patch antenna. The EBG parameters used are: UC 10 mm × 10 mm, EBG patch 8.5 mm × 8.5 mm, vias radius 0.2 mm, substrate thickness 1.5748 mm (EBG surface in the middle), and all dielectric layers are FR-4 materials.

Conventional rectangular microstrip patch antennas operate at the fundamental TM_{10} mode. As was discussed in Section II, this also seems to be the case for a patch antenna over an EBG substrate, except with a reduced wavelength as observed in the dispersion diagram. In this section, the resonant frequency of a rectangular patch antenna on top of an EBG (mushroom) structure is investigated through the use of the Zeland IE3D full-wave solver (moment method code). An open-circuit microstrip line at the EBG surface is proximity-coupled to the radiating patch. Resonant frequencies for a set of square radiation patch lengths (10, 20, 30, 40, 50, and 60 mm) are found from the return loss dip under a frequency sweep.

Since the fundamental patch resonant frequency depends mostly on the propagation wavelength λ of the substrate, the corresponding linear dimension of patch antenna is close to half-wavelength. Both the UC and FCS-EM analyses are used to produce the antenna resonant length based on a half-wavelength approximation. The results are shown in Fig. 3. The FCS-EM analysis is found in very good agreement with the 3-D antenna simulation. It confirms the validity of the half-wavelength transmission line approach and the accuracy of the modal analysis. A discrepancy is observed for the UC-EM analysis when the patch width becomes narrow compared to an EBG UC length.

As an example, for a patch size of 10 mm × 10 mm, both full-wave 3-D simulation and FCS-EM modal analysis show that the patch resonant frequency is about 2.92 GHz (way into the parallel-plate bandgap zone), while the UC model shows that the EBG patch antenna frequency is 2.41 GHz (for a wavelength of 20 mm). This discrepancy implies that the UC parallel-plate cavity (UC-EM) model is no longer appropriate in this case since fringe fields at the EBG patch antenna edge become dominant and are not confined below the radiation patch with vertical polarization. Therefore, the inaccuracy of the cavity mode becomes noticeable when the patch antenna size is close to or even smaller than the mushroom patch size. In this case, the antenna resonant frequency is mostly determined by the local EBG profile similar to the case of a strip dipole.

TABLE I
Resonant Frequencies of a Square Patch Antenna

Patch Dimension (mm^2)	Plain Antenna Resonant Freq [GHz]	EBG Antenna Resonant Freq [GHz]
10x10	6.29	2.92
20x20	3.32	2.15
30x30	2.25	1.67
40x40	1.71	1.27
50x50	1.38	1.03
60x60	1.15	0.85

Since there is no suitable wavelength within the bandgap zone, the EBG patch antenna is not an effective radiator at its bandgap region and the AMC property of EBG substrate corresponding to the EBG resonance is not useful for antenna radiation, as a result of strong mutual coupling between radiation patch element and EBG texture.

The resonant frequencies of a square patch antenna with or without EBG surface underneath are obtained using a full 3-D simulator (Zeland IE3D) and are shown in Table I. It is seen that an EBG patch antenna has a lower resonant frequency as compared to a patch antenna without EBG insert. Also, the difference of the two in resonant frequency increases as the size of the patch antenna becomes smaller. Furthermore, the resonant frequency of a normal patch is 35% higher than that of an EBG patch when their patch size is 60 mm × 60 mm. However, when the radiation patch size decreases to 10 mm × 10 mm, it is a few times higher. It indicates that the slow-wave effect becomes stronger when EBG patch antenna approaches its inherent bandgap, which is also shown in the UC eigenanalysis in Fig. 3. Table I also suggests that at a chosen operating frequency, the patch size can be much smaller with an EBG surface as was reported previously [20], [21].

The results in Fig. 3 suggest that the increase in patch width will decrease the transmission line wavelength and the patch length, which is true even for a normal microstrip patch without EBG surface. An example of wavelength versus frequency within the first passband is shown in Fig. 4 for various microstrip line widths. The simulation is based on the FCS-EM modal analysis. For comparison, the results from a UC-EM modal analysis (infinite large line width) are also shown. The FCS-EM modal analysis agrees better with the UC eigenanalysis for a wide strip. For a narrower strip, as mentioned before, the fringe fields at the strip edge are more significant and the FCS-EM modal provides a more accurate dispersion curves than the UC-EM model. It is noted that the results change very little when the strip width increases from 20 to 60 mm. The results confirm that when the strip is sufficiently wide (as the

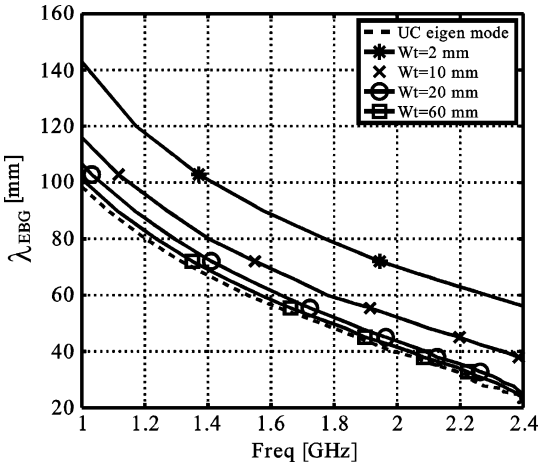

Fig. 4. Wavelength of the fundamental mode verse frequency for a microstrip line above an EBG surface with various width.

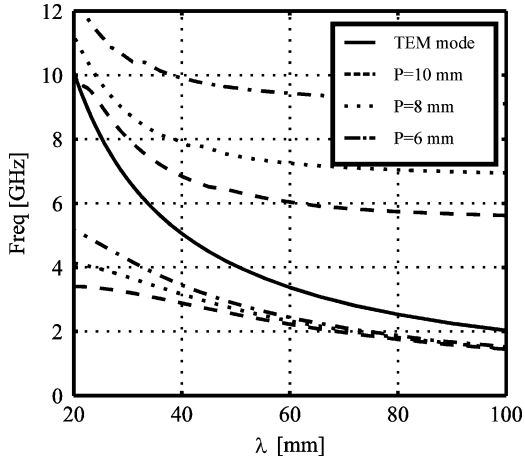

Fig. 5. Dispersion diagrams of mushroom-like EBGs for different UC lengths at 81% filling factor (dashed lines: 10 mm, dotted lines: 8 mm, dash-dot lines: 6 mm, and solid line: parallel-plate TEM mode).

case of a patch), its width and the location of the strip relative to the EBG surface profiles are insignificant to the phase constant (patch antenna length) and the UC-EM cavity model works well even with an EBG surface insertion. It is observed from Fig. 4 that the FCS-EM modal analysis can also be used to design a half-wavelength thin dipole antenna above an EBG surface.

IV. Parametric Analysis of Different Types of EBG Back Patch Antenna

The EBG patch antenna characteristics are determined by both the EBG parameters and the radiation patch dimensions. Only the mushroom EBG structure is presented here. Uniplanar compact photonic bandgap (UC-PBG) structure [3] had been proposed for microwave applications [26], [27]. The main advantage is that its pattern requires no additional vertical vias and could be useful for certain applications. However, for patch antenna applications, through some parametric studies, different shapes of EBG patterns including UC-PBG or hexagon shape seem to have no particular radiation performance advantage over the rectangular mushroom structure.

As shown in Section III, the dispersion diagram of the EBG structure with a metal plate cover reveals the radiation mode mechanism of the EBG patch antenna, and successfully predicts the antenna resonant frequency. Parametric analysis of the EBG surface effects on the transmission-line wavelength is presented in this section. The results provide an engineering guideline for designing, tuning, and optimizing microstrip antenna radiation over general EBG substrates and also help to understand EBG surface effects to planar radiation elements.

The electromagnetic bandgap and slow-wave factor of the first propagation mode are determined by the EBG patch dimension (A), the spacing between EBG patches (S), EBG substrate thickness $(T_{\rm EBG})$, the distance between the radiation patch and EBG surface $(T_{\rm ant})$, and the substrate materials. Once these parameters are determined, the antenna resonant frequency can be found from the dispersion diagram with good accuracy.

The dispersion diagram for different mushroom-like EBG UC sizes $P = A + S$ are shown in Fig. 5. The ratio of the EBG patch to the UC (A/P) is kept at 0.9 (81% filling). Roger-5880

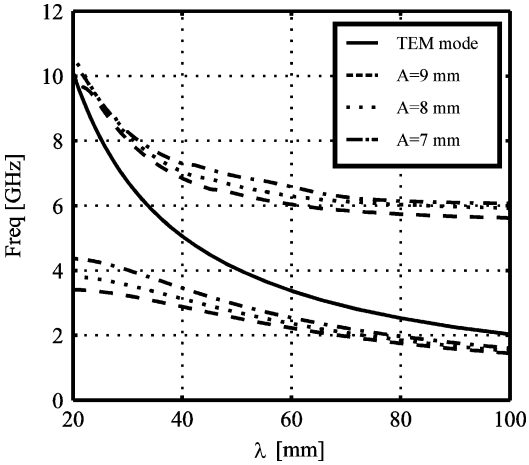

Fig. 6. Dispersion diagrams of mushroom-like EBGs for different EBG conducting plate size with a 10-mm UC (dashed lines: 9 mm, dotted lines: 8 mm, dash-dot lines: 7 mm, and solid line: parallel-plate TEM mode).

substrate ($\varepsilon_r = 2.2$ and $\delta_{\rm loss} = 0.0009$) is assumed, but the observation should be general enough for other types of materials. The substrate thickness is 1.5748 mm (62 mil) with EBG patch in the middle. It is found that by scaling down the EBG UC dimension, the bandgap width increases and shifts higher, which can be explained by the theory of a capacitor-loaded periodic transmission line [28]. The fundamental mode that is closely related to the radiation mode is insensitive to the EBG UC except near the bandgap zone.

The dispersion diagrams for different EBG patch sizes A (same UC size P) are shown in Fig. 6. It is seen that the EBG patch size has an insignificant effect on the mode characteristics. For a smaller EBG patch, the coupling capacitance reduces and the slow-wave factor is smaller (larger wavelength).

The comparison of dispersion curves for several different top dielectric layer heights $T_{\rm ant}$ is shown in Fig. 7. It is observed that a smaller top layer thickness corresponds to a larger bandgap and a larger slow-wave factor. It is seen that when the height is large enough, the dispersion curves merge to that of the parallel-plate TEM mode, implying that the EBG effect is diminishing.

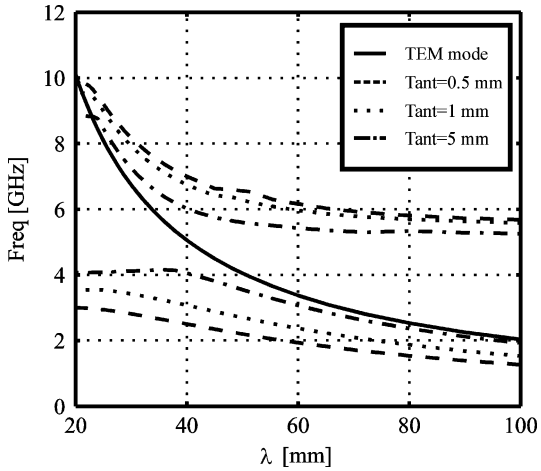

Fig. 7. Dispersion diagrams of mushroom-like EBGs for various top-layer heights (dashed lines: 0.5 mm, dotted lines: 1 mm, dash-dot lines: 5 mm, and solid line: parallel-plate TEM mode).

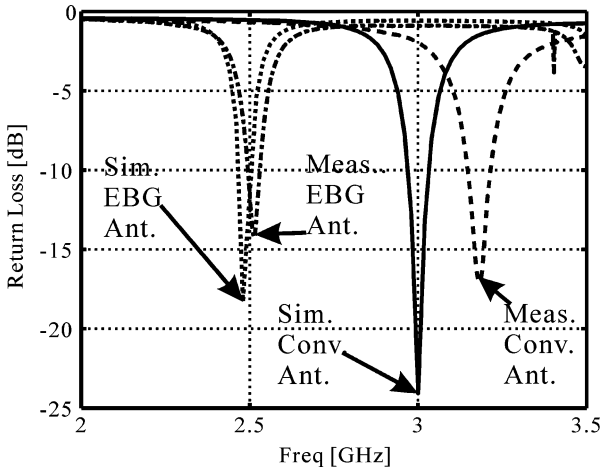

Fig. 9. Return loss comparison of a patch antenna on a normal or an EBG substrate.

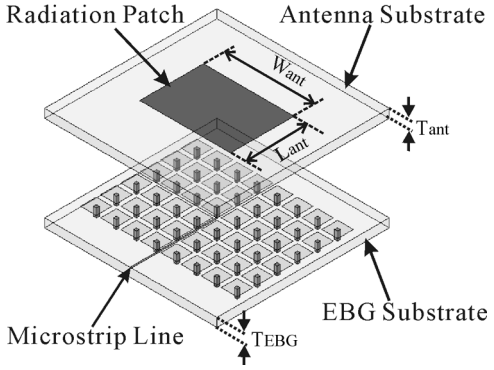

Fig. 8. Rectangular patch antenna over a mushroom-like EBG substrate proximity-fed by a microstrip line.

As a result, in this case, the EBG surface tends to act as perfect electric conductor rather than a magnetic conductor.

V. Prototype of a Patch Antenna Above an EBG Surface

A prototype of linear-polarized microstrip antenna on a mushroom-like EBG substrate is fabricated and tested. Antenna return loss and radiation pattern are investigated and compared to those of a conventional microstrip patch antenna.

The configuration of a microstrip antenna with an EBG substrate is depicted in Fig. 8. The antenna structure includes two 0.7874-mm-thick (31 mil), 70-mm-long, and 85-mm-wide dielectric FR4-epoxy layers, with parameters $\varepsilon_r = 4.6$ and loss tangent 0.01. The EBG patch arrays with 6×8 mushroom-like UCs are in the middle of the cavity. The rectangle radiation patch is etched above the top FR4 substrate, with dimension $L =$ 22.14 mm and $W = 31.59$ mm. The EBG UC size is 7 mm, EBG patch dimension is 4.5 mm $\times$ 4.5 mm, and grounding vias radius 0.2 mm. Dispersion diagram obtained from the modal analysis is already shown in Fig. 2. It predicts that the wavelength is about 42 mm ($L = 21$ mm) at 2.5 GHz and serves as the initial design. All the EBG planar texture and vertical vias are designed and fabricated in the bottom FR4 substrate. In addition, a 50 Ω open-circuited microstrip line (1.2 mm in width) is also printed on the same surface as the EBG patches, and proximity-coupled to the upper radiation patch. Two dielectric substrate layers are finally laminated together by multilayer PCB technique to form a low-profile planar antenna. The 3-D full-wave IE3D simulation is used to fine-tune the patch length.

The simulated and measured results of the return loss ($|S_{11}|$) are given in Fig. 9. A conventional microstrip antenna with the same size radiation patch is also designed and tested as a reference. The simulation predicts the resonant frequency at 3 GHz, while the measurement shows the resonance at 3.18 GHz, for a normal patch antenna. In contrast, the resonant frequency of an EBG patch antenna is predicted at 2.48 GHz by 3-D full-wave IE3D simulations (with $L =$2 2.14 mm) and at 2.52 GHz by measurement. Both the simulation and measurement results show that after introducing EBG patterns in the bottom dielectric substrate, the resonant frequency of patch antenna and the bandwidth both decrease. The discrepancies between simulations and measurements are basically due to the tolerance of PCB fabrication. The decrease in resonant frequency for an EBG antenna is due to the capacitive and inductive loadings of the EBG profiles under the patch. The decrease in bandwidth is probably due to fact that the ground backing of the patch antenna is effectively moved up to the EBG surface and reduces the effective substrate thickness, and the patch antenna bandwidth is roughly proportional to the substrate thickness.

The radiation patterns of an EBG patch antenna are measured in an anechoic chamber room at 2.5 GHz. Both simulated and measured E- and H-plane patterns are shown in Figs. 10 and 11, respectively. The main beam direction at the first resonant frequency 2.5 GHz is in broadside direction normal to antenna surface, and the corresponding antenna gain is about 3.75 dBi. The backward radiation of EBG patch antenna is at around -15 dBi, which is at about the same level of a conventional patch antenna. In general, comparison between simulation and measurement shows very good agreement. The radiation patterns for an EBG patch are similar to those of a normal microstrip patch antenna at its fundamental mode.

The effects of the EBG UC on the radiation characteristics of a patch antenna are investigated though IE3D full-wave simulation. Several cases of EBG loadings are used to investigate their

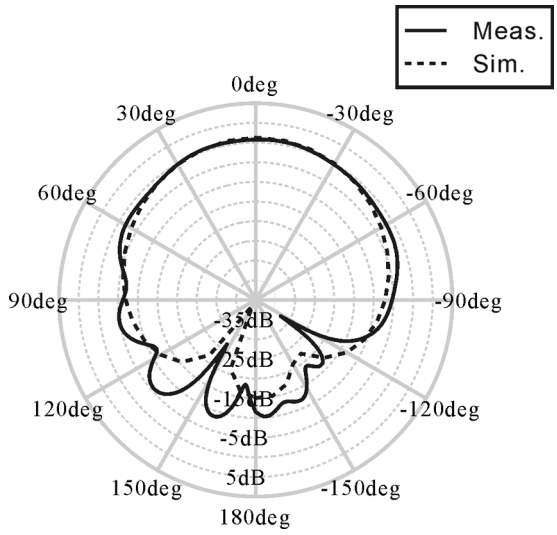

Fig. 10. E-plane radiation patterns of an EBG patch antenna at 2.5 GHz. The dashed line is corresponding to simulation and the solid line is corresponding to measurement.

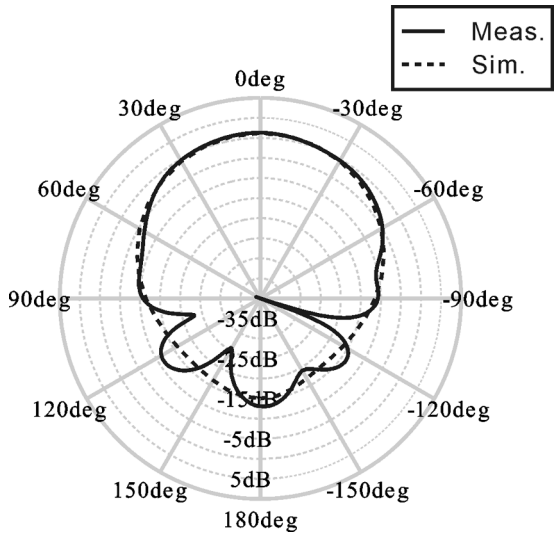

Fig. 11. H-plane radiation patterns of an EBG patch antenna at 2.5 GHz. The dashed line is corresponding to simulation and the solid line is corresponding to measurement.

effects on a proximity-coupled microstrip patch antenna. The results are shown in Table II. Note that EBG UC size is noted as "P" and the EBG patch length is "$A = P - S$." The last row in Table II corresponds to the case in Figs. 9–11. For each case, the feeding line inset length is readjusted slightly to obtain best matching. The resonant frequencies are basically determined by antenna and EBG structures, and invariant with feeding offsets.

The results show that the main beam (broadside), gain, directivity, and radiation efficiency are at about the same level as a conventional patch antenna but with a smaller bandwidth. The results also show that with the increase of the EBG UC size (P) (higher metal density), the resonant frequency decreases, as predicted by the slow-wave factor increase in modal analysis shown in Section IV, and therefore, the antenna resonant frequency will decrease. As mentioned in Section IV, the EBG surface can

TABLE II
COMPARISON OF ANTENNA PARAMETERS WITH DIFFERENT EBG PERIODICITY—SPACING FOR OPTIMAL TUNING

Unit cell dimension	Resonant frequency (GHz)	Bandwidth (MHz)	Gain (dB)	Direct. (dB)	Efficiency
Normal (no EBG)	3.0	60.3	3.88	6.42	55.7%
P=7mm *S*=1.5mm	2.31	28.0	2.94	5.67	53.1%
P=6mm *S*=1.5mm	2.34	28.0	3.01	5.73	53.5%
P=5mm *S*=1.5mm	2.47	32.6	3.50	5.82	57.9%
P=7mm *S*=2mm	2.50	30.8	3.20	5.75	55.6%
P=7mm *S*=2.5mm	2.49	33.6	3.51	5.83	58.6%

be treated as capacitive/inductive loadings to a microstrip line above. The increase in capacitance reduces the wavelength and increases the patch resonant frequency. A 23.3% frequency reduction is observed with $P = 7$ mm and $S = 1.5$ mm compared to the unloaded case. In such a case, the patch antenna length is reduced to 0.376λ from close to 0.5λ. The EBG patch adjacent spacing S is also varied to verify the frequency shift properties described in Section IV. By comparing the three cases, $S = 2.5$, 2, and 1.5 mm with $P = 7$ mm fixed, the resonant frequency varied from 2.5 to 2.3 GHz. Since the EBG capacitance also increases while adjacent patch spacing reduces, the size reduction is expected. The bandwidth reduction seen in Table II is due to the fact that the effective ground plane moves closer to the patch antenna and the Q factor increases.

VI. CONCLUSION

A microstrip patch antenna over an EBG substrate was investigated in this paper. The radiation characteristics of the antenna fundamental mode were found similar to the fundamental TM_{10} mode of a conventional microstrip patch antenna. Modal analyses for a microstrip line above an EBG surface were developed to predict the antenna fundamental resonance and provide useful physical insights of the coupling effect between the EBG surface and the radiation element. The EBG effects were analyzed parametrically. The results show that for a mushroom-like EBG substrate, the bandgap spectrum will change from high-pass to low-pass, when a metal plate is added on top, and the EBG surface tends to behave like a periodically loaded capacitor/inductor in the first passband. It was also found that for an EBG patch antenna operated at the fundamental mode, the patch size is significantly smaller than the size of a normal microstrip patch. This property could be useful for antenna miniaturization.

Furthermore, the AMC is not found for a radiation patch over an EBG substrate due to the fact that strong near-field coupling between EBG substrate and top planar conducting patch alters bandgap and EBG resonant characteristics. Although not discussed here, the design method is also applicable to the strip dipole case. A prototype of a microstrip line proximity fed to a patch antenna was fabricated and tested to verify the analysis.

REFERENCES

[1] K.-L. Wong, *Compact and Broadband Microstrip Antennas*. New York: Wiley, 2002.

[2] D. Sievenpiper, L. Zhang, R. F. J. Broas, N. G. Alexopolous, and E. Yablonovitch, "High-impedance electromagnetic surfaces with a forbidden frequency," *IEEE Trans. Microw. Theory Tech.*, vol. 47, no. 11, pp. 2059–2074, Nov. 1999.

[3] F.-R. Yang, K.-P. Ma, Y. Qian, and T. Itoh, "A uniplanar compact photonic-bandgap (UC-PBG) structure and its applications for microwave circuit," *IEEE Trans. Microw. Theory Tech.*, vol. 47, no. 8, pp. 1509–1514, Aug. 1999.

[4] V. Veselago, "The electrodynamics of substances with simultaneously negative values of ε and μ," *Soviet Phys. Uspekhi*, vol. 10, no. 4, pp. 509–514, 1968.

[5] R. A. Shelby, D. R. Smith, and S. Schultz, "Experimental verification of a negative index of refraction," *Science*, vol. 292, no. 5514, pp. 77–79, Apr. 2001.

[6] C. Caloz and T. Itoh, "Transmission line approach of left-handed (LH) materials and microstrip implementation of an artificial LH transmission line," *IEEE Trans. Antennas Propag.*, vol. 52, no. 5, pp. 1159–1166, May 2004.

[7] A. Lai, C. Caloz, and T. Itoh, "Composite right/left-handed transmission line metamaterials," *IEEE Microw. Mag.*, vol. 5, no. 3, pp. 34–50, Sep. 2004.

[8] G. V. Eleftheriades, A. K. Iyer, and P. C. Kremer, "Planar negative refractive index media using periodically L-C loaded transmission lines," *IEEE Trans. Microw. Theory Tech.*, vol. 50, no. 12, pp. 2702–2712, Dec. 2002.

[9] R. Gonzalo, P. De Maagt, and M. Sorolla, "Enhanced patch-antenna performance by suppressing surface waves using photonic-bandgap substrates," *IEEE Trans. Microw. Theory Tech.*, vol. 47, no. 11, pp. 2131–2138, Nov. 1999.

[10] J. S. Colburn and Y. Rahmat-Samii, "Patch antennas on externally perforated high dielectric constant substrates," *IEEE Trans. Antennas Propag.*, vol. 47, no. 12, pp. 1785–1794, Dec. 1999.

[11] F. Yang and Y. Rahmat-Samii, "Microstrip antennas integrated with electromagnetic band-gap (EBG) structures: A low mutual coupling design for array applications," *IEEE Trans. Antennas Propag.*, vol. 51, no. 10, pp. 2936–2946, Oct. 2003.

[12] Z. Li and Y. Rahmat-Samii, "PBG, PMC and PEC ground planes: A case study of dipole antennas," in *Proc. IEEE Antennas Propag. Soc. Int. Symp. Dig.*, Jul. 2000, vol. 2, pp. 674–677.

[13] D. J. Kern, D. H. Werner, A. Monorchio, L. Lanuzza, and M. J. Wilhelm, "The design synthesis of multiband artificial magnetic conductors using high impedance frequency selective surfaces," *IEEE Trans. Antennas Propag.*, vol. 53, no. 1, pp. 8–17, Jan. 2005.

[14] N. Christopoulos, G. Goussetis, A. P. Feresidis, and J. C. Vardaxoglou, "Metamaterials with multiband AMC and EBG properties," in *Proc. Eur. Microw. Conf.*, Oct. 2005, vol. 1, pp. 77–79.

[15] F. Yang and Y. Rahmat-Samii, "Reflection phase characterizations of the EBG ground plane for low profile wire antenna applications," *IEEE Trans. Antennas Propag.*, vol. 51, no. 10, pp. 2691–2703, Oct. 2003.

[16] J. Bell and M. Iskander, "A low-profile archimedean spiral antenna using an EBG ground plane," *IEEE Antennas Wireless Propag. Lett.*, vol. 3, pp. 223–226, 2004.

[17] A. P. Feresidis, G. Goussetis, S. Wang, and J. C. Vardaxoglou, "Artificial magnetic conductor surfaces and their application to low-profile high-gain planar antennas," *IEEE Trans. Antennas Propag.*, vol. 53, no. 1, pp. 209–215, Jan. 2005.

[18] S. Pioch and J.-M. Laheurte, "Size reduction of microstrip antennas by means of periodic metallic patterns," *Electron. Lett.*, vol. 39, no. 13, pp. 959–961, Jun. 2003.

[19] S. Pioch and J.-M. Laheurte, "Parametric study of compact flat antennas based on periodic patterns," *Microw. Opt. Tech. Lett.*, vol. 40, no. 4, pp. 311–314, Jan. 2004.

[20] M. Ermutlu, C. Simovski, M. Karkkainen, P. Ikonen, S. Tretyakov, and A. Sochava, "Miniaturization of patch antennas with new artificial magnetic layers," in *Proc. IEEE Int. Workshop Antenna Technol.: Small Antennas Novel Metamaterials (IWAT)*, March 2005, pp. 87–90.

[21] K. Z. Rajab, R. Mittra, and M. T. Lanagan, "Size reduction of microstrip antennas using metamaterials," in *Proc. IEEE Antennas Propag. Soc. Int. Symp. Dig.*, Jul. 2005, vol. 2B, pp. 296–299.

[22] H. Yang and J. Liang, "Analysis of a proximity coupled patch antenna on metalized EBG substrates," in *IEEE Antennas Propag. Soc. Int. Symp.*, Albuquerque, NM, Jul. 2006, pp. 2287–2290.

[23] H. Mosallaei and K. Sarabandi, "Antenna miniaturization and bandwidth enhancement using a reactive impedance substrate," *IEEE Trans. Antennas Propag.*, vol. 52, no. 9, pp. 2403–2414, Sep. 2004.

[24] H. Mosallaei and K. Sarabandi, "Design and modeling of patch antenna printed on magneto-dielectric embedded-circuit metasubstrate," *IEEE Trans. Antennas Propag.*, vol. 55, no. 1, pp. 45–52, Jan. 2007.

[25] S. Pioch and J.-M. Laheurte, "Low profile dual-band antenna based on a stacked configuration of EBG and plain patches," *Microw. Opt. Tech. Lett.*, vol. 44, no. 3, pp. 207–209, Feb. 2005.

[26] R. Coccioli, F.-R. Yang, K.-P. Ma, and T. Itoh, "Aperture-coupled patch antenna on UC-PBG substrate," *IEEE Trans. Microw. Theory Tech.*, vol. 47, no. 11, pp. 2123–2130, Nov. 1999.

[27] F.-R. Yang, K.-P. Ma, Y. Qian, and T. Itoh, "A novel TEM waveguide using uniplanar compact photonic-bandgap (UC-PBG) structure," *IEEE Trans. Microw. Theory Tech.*, vol. 47, no. 11, pp. 2092–2098, Nov. 1999.

[28] D. M. Pozar, *Microwave Engineering*, 3rd ed. New York: Wiley, 2005, p. 377.

Jing Liang (S'06) received the B.Eng. degree in information science and electronic engineering from the Zhejiang University, Hangzhou, China, in 2003. Currently, he is working towards the Ph.D. degree in electrical and computer engineering at the University of Illinois at Chicago, Chicago.

His research interests include low-profile electrically small antennas for wireless communication, reconfigurable antennas in RF systems, metamaterials interactions with antennas and RF passive components, and antenna array analysis and synthesis for direction finding systems.

Hung-Yu David Yang (M'88–SM'93–F'00) received the Ph.D. degree in electrical engineering from the University of California at Los Angeles, Los Angeles, in 1988.

He has been with the Electrical and Computer Engineering Department, University of Illinois at Chicago, Chicago, since 1992 and is now a Professor. He has published over 120 journal and conference papers and holds six U.S. patents. In 2001, he took a sabbatical leave to wireless industry, working on passive component designs of radio-frequency integrated circuits (RFIC), the front-ends radio components, such as antennas, filters, baluns, and other passives. His current research efforts include novel wireless RF front-end antennas and passives, theory of 3–D substrate metallization including EBG and metamaterials.

Mr. Yang has been the Editor-in-Chief of *Electromagnetics* since 1997. He is a member of URSI commission B and Sigma Xi. He has been a technical program committee member of the IEEE International Microwave Symposium since 1994. He also serves on the editorial board of various professional journals.